Published in final edited form as:
J Biomed Mater Res A. 2010 January ; 92(1): 152–163. doi:10.1002/jbm.a.32343.

Fibrin-based tissue engineering scaffolds enhance neural fiber sprouting and delays the accumulation of reactive astrocytes at the lesion in a subacute model of spinal cord injury†

Philip J Johnson[1], **Stanley R Parker**[1], and **Shelly E. Sakiyama-Elbert**[1,2,3,*]

[1]Department of Biomedical Engineering, Washington University, St. Louis, MO 63130, USA

[2]Division of Plastic and Reconstructive Surgery, Department of Surgery, Washington University School of Medicine, St. Louis, MO 63110, USA

[3]Center for Materials Innovation, Washington University, St. Louis, MO 63130, USA

Abstract

The purpose of this study was to evaluate the effects of fibrin scaffolds on subacute rat spinal cord injury (SCI). Long Evans rats were anesthetized and underwent a dorsal hemisection injury, two weeks later the injury site was re-exposed, scar tissue was removed, and a fibrin scaffold was implanted into the wound site. An effective method for fibrin scaffold implantation following subacute SCI was investigated based on the presence of fibrin within the lesion site and morphological analysis 1 week after implantation. Pre-polymerized fibrin scaffolds were found to be present within the lesion site 1 week after treatment and were used for the remainder of the study. Fibrin scaffolds were then implanted for 2 and 4 weeks, after which spinal cords were harvested and evaluated using markers for neurons, astrocytes, and chondroitin sulfate proteoglycans. Compared to untreated control, the fibrin-treated group had significantly higher levels of neural fiber staining in the lesion site at 2 and 4 weeks after treatment, and the accumulation of glial fibrillary acidic protein (GFAP) positive reactive astrocytes surrounding the lesion was delayed. These results show that fibrin is conducive to regeneration and cellular migration, and illustrates the advantage of using fibrin as a scaffold for drug delivery and cell-based therapies for SCI.

Keywords

nerve regeneration; glial scar; CNS scaffold; spinal cord regeneration

Introduction

Traumatic SCI results in the loss of motor and sensory pathways, which has devastating consequences for injured patients. Spontaneous regeneration of adult mammalian spinal cord neurons is limited by inhibitory environmental factors, both those intrinsic to the adult spinal cord and those induced by the injury. These environmental factors, including myelin-associated inhibitors, the glial scar and cystic cavity formation, create a physical and molecular barrier to regeneration of injured spinal tissue1›2.

†No benefit of any kind will be received either directly or indirectly by the authors.

*To whom correspondence should be addressed: Shelly Sakiyama-Elbert, Department of Biomedical Engineering, Washington University, Campus Box 1097, One Brookings Drive, St. Louis, MO 63130, Telephone: (314) 935-7556, sakiyama@wustl.edu

Primary injury to the spinal cord results in the focal destruction of neural tissue caused by direct mechanical trauma. Over time, the primary injury propagates a progressive series of secondary injuries, which exacerbate the damage to the spinal cord3. Finally, a glial scar forms at the border of the lesion site that serves as an inhibitory barrier to axonal regeneration. The progression of SCI over time means that the cellular and molecular makeup of the lesion immediately following injury is drastically different than that found weeks later. Therefore, when considering a therapeutic intervention for SCI, it is important to consider at what time point post injury the intervention will be implemented. Ideally in a clinical setting treatment would be administered acutely (<24hrs) following injury to minimize the propagation of secondary injury. However, tissue engineering therapeutic strategies for SCI will most likely be implemented at a time when the secondary injury cascade has begun.

Despite the limited likelihood of acute implementation of tissue engineered therapies for SCI, many studies have focused on tissue engineering interventions for SCI at acute time points following injury (minutes and hours). However, investigation of experimental therapies at a time point when the injury has stabilized allows the therapy to be evaluated under conditions that are more similar to those that would be applicable for a broader patient group. Furthermore, delayed intervention provides a more consistent model for the evaluation of treatment efficacy by reducing the number of experimental variables. To this end, our lab in previous studies evaluated a dorsal hemisection SCI model over an 8 week time course (unpublished data). From the results of this study it was determined, based on injury size and glial scar formation that the lesion site following dorsal hemisection stabilized at 2 weeks post injury.

The molecular and cellular makeup of the injury environment has been shown to be important for endogenous regeneration in most mammalian tissues 4. Given the appropriate environment, damaged neural tissue of the central nervous system (CNS) is capable of limited regeneration 5،6. To modulate the environment following injury, biomaterial scaffolds to “bridge the gap” or reconstruct damaged CNS tissue following SCI are being developed with characteristics that promote the migration of support cells into the biomaterial to enhance axonal regeneration7.

Migration of support cells into the injured area is essential for providing an extracellular milieu that is conducive to regeneration. Using *in situ* forming agarose scaffolds, Jain *et al.* found that failure to promote infiltration of support cells into the scaffold resulted in an absence of axonal regeneration. Moreover, it was shown that by introducing soluble growth factors both cell migration and axonal penetration was enhanced 8. Other groups have attempted to bypass the need for endogenous cell migration by using scaffolds seeded with Schwann cells prior to implantation. However the inability to maintain the viability of the exogenous cells resulted in little therapeutic effect 9. Stokols *et al.* found that axonal regeneration within channels of their freeze-dried agarose scaffolds correlated with integration of endogenous Schwann cells and vascular endothelial cells 10. Likewise, Woerly *et al.* found in addition to the infiltration of support cells, the presence of vasculature within the scaffold was associated with increased axonal regeneration 11.

Fibrin is a desirable biomaterial scaffold for nerve regeneration based on its role in wound repair and tissue reconstruction. Fibrin has also been studied extensively as a biomaterial. Clinically, it has been used as a tissue adhesive for skin repair12. In neural tissue engineering, it has been used as a matrix to fill nerve guidance tubes implanted following sciatic nerve injury and was shown to promote axonal regeneration and cell migration13. Fibrin scaffolds have also been used in acute studies of complete spinal cord transection, and were found to elicit increased neural fiber sprouting at early time points when compared to

controls14. Fibrin scaffolds can be modified covalently to form an affinity-based delivery system for the controlled delivery of neurotrophins15,16.

In this study the feasibility of using a fibrin scaffold to treat a subacute (2 weeks post injury) SCI model in rats was investigated. A subacute dorsal hemisection model was used to evaluate the ability of fibrin to promote neural fiber sprouting and increase migration of neural support cells into the lesion site following injury.

Methods

Fibrin Scaffold Preparation and Polymerization Method

All materials were purchased from Fisher Scientific (Pittsburgh, PA) unless otherwise noted. Fibrin scaffolds were made as described previously17 by mixing the following components: human plasminogen-free fibrinogen containing Factor XIII (10 mg/mL, Sigma, St. Louis, MO), fluorescently labeled human fibrinogen (0.4 mg/mL, Invitrogen, Carlsbad, CA), $CaCl_2$ (5mM), and thrombin (12.5 NIH units/mL, Sigma) in Tris-buffered saline (TBS, 137 mM NaCl, 2.7 mM KCl, 33 mM Tris, pH 7.4). The degradation of fibrin scaffolds was evaluated for two different polymerization methods: pre-polymerization and *in situ* polymerization. Pre-polymerized fibrin scaffolds (10 μL in volume) were formed by ejecting the polymerization mixture from a 20 μL pipette tip such that a spherical scaffold formed on the tip of the pipette. The sphere was then allowed to polymerize on the pipette tip for 5 min prior to implantation into the injury site. *In situ* polymerized scaffolds were formed by ejecting the polymerization solution from a pipette tip directly into the injury site and allowing it to polymerize in the injury site.

In-vivo Studies - Dorsal Hemisection Subacute SCI model

All experimental procedures on animals complied with the Guide for the Care and Use of Laboratory Animals and were performed under the supervision of the Division of Comparative Medicine at Washington University. Long-Evans female rats (250-275 g, Harlan, Indianapolis, IND) were anesthetized using 4% isoflurane gas (Vedco Inc., St Josephs, MO). The skin and muscle overlying the spinal column were incised and dissected away from the spinal column. Clamps were attached to the spinous processes and a rigid frame was used to immobilize the spinal column. A dorsal laminectomy was performed using fine rongeurs at level T-9 to expose the spinal cord. A lateral slit in the dura was made, and microdissection scissors (Fine Science Tools, Forest City, CA) mounted to a micromanipulator were lowered into the spinal cord 1.2 mm from the dorsal spinal cord surface. Using the microdissection scissors, a lateral incision was made to form a complete dorsal hemisection of the spinal cord. Finally the microdissection scissors were run through the incision to assure the hemisection was complete. The cord was then covered with a piece of artificial dura, the muscles were sutured with degradable sutures and the skin was stapled close. Two weeks following initial injury, the injury site was re-exposed, and scar tissue was removed from the wound site.

To determine an effective method for implantation and polymerization of fibrin scaffolds in the lesion site, two methods of implantation were evaluated. The scaffolds were either allowed to polymerize partially into 10 μL beads for 5 min at room temperature prior to implantation (pre-polymerized, n = 3) or the mixture of fibrinogen and thrombin was injected into the wound site for *in situ* polymerization (*in situ*, n = 3). Controls received a sham operation with the same injury and removal of scar tissue with no fibrin scaffolds (n=3). The wound was then closed and 1 week following implantation, the rats were euthanized, and their spinal cords were harvested to assay for the presence of fluorescently labeled fibrin.

Pre-polymerized scaffolds were then used to evaluate the morphological and behavioral effect on subacute SCI at specific time points following treatment (2 and 4 weeks). Groups receiving fibrin scaffolds (n=6 for 2 weeks, and n=6 for 4 weeks) and controls receiving the same injury with removal of scar tissue (n=6 for 2 weeks, and n=6 for 4 weeks) were evaluated at 2 and 4 weeks (total of 24 rats, n=6 for each group at each time point).

Animals were given cefazolin (15 mg/kg, twice a day) for five days following each surgical procedure as a prophylactic against urinary tract infections. Bladders were expressed manually twice a day until they regained bladder control approximately 5 to 6 days post initial injury. The animals were euthanized 1, 2, or 4 weeks post treatment. After transcardial perfusion using 4% paraformaldehyde (Sigma), spinal cords were dissected and post fixed in 4% paraformaldehyde solution overnight. The cords were then cryoprotected in a 30% sucrose solution in phosphate buffered saline (PBS) in preparation for processing. The spinal cord was embedded in Tissue-Tek OCT compound Mounting Media (Sakura Finetek, Torence, CA) and cut into 20 μm sagittal sections using a cryostat.

Immunohistochemistry

Immunohistochemistry was used to analyze morphological aspects of each experimental group. Sections were washed with phosphate-buffered saline and permeabilized with 0.1% Triton X-100 for 5 min. After washes in PBS, the sections were blocked with 10% bovine serum albumin (BSA, Sigma) and 2% normal goat serum (NGS, Sigma). Primary antibodies against glial fibrillary acidic protein (GFAP, rabbit polyclonal, recognizing astrocytes, 1:4, ImmunoStar, Hudson, WI), neuronal class III β-tubulin (Tuj1, mouse monoclonal, recognizing neurons, 1:200, Covance Research Products, Berkeley, CA), ED-1 (mouse monoclonal, recognizing macrophages and microglia, 1:100, Serotec, Oxford, UK) and NG2 chondroitin sulfate proteoglycan (CSPG) (NG2, rabbit polyclonal, 1:200, Chemicon) were used to evaluate sections. Each sagittal section was double stained with either Tuj1 and GFAP, ED1 and GFAP, or NG2 and Tuj1. Finally, appropriate secondary antibodies (Alexa Fluor 488, 555, and 647 conjugated, 1:300 Invitrogen, Carlsbad, CA) with 2% NGS were used and each section was stained with Hoechst nuclear stain .

Quantification of Neural Fiber Density, Astrocyte Density, CSPG Density, and Lesion Area

Each spinal cord section was imaged at 40x magnification using an Olympus IX70 microscope (Olympus America, Melville, NY) and Magnafire Camera (Optronics, Goleta, CA). Imaging resulted in multiple 40x images that spanned the entire spinal cord section and that were later spliced together using Photoshop (Adobe, San Jose, CA) to yield a complete picture of the lesion and surrounding intact cord. The density of neural fibers within the lesion that stained positive for Tuj1 was quantified from 6 serial sections spaced 200μm apart from each rat. The density of Tuj1 staining was quantified inside the lesion area using the binary image processing software Ia32 (Leco, St. Joseph, MI). The lesion was defined as the space within the GFAP-positive border and a straight line connecting the dorsal surface of the injured spinal cord (Figure 1). An intensity threshold was set so that only Tuj1 positive neuronal fibers were quantified within the lesion. The area of positive Tuj1 staining within the lesion (the number of pixels in which the intensity was above the set intensity threshold) was divided by the total number of pixels within the lesion to yield the neural fiber density.

The density of GFAP staining of astrocytes and the presence of NG2 was quantified inside the white matter that bordered the lesion for all experimental groups. Four 200x magnification images of the white matter surrounding the lesion site were taken from 6 serial sections spaced 200μm apart for each rat. Two images were taken of the intact white matter region bordering the rostral side of the lesion (as defined by GFAP staining) and two

images were taken of the intact white matter region bordering the caudal side of the lesion (Figure 1A). The images were then analyzed using the Ia32 software. An intensity threshold was set so that only areas positive for GFAP or NG2 were quantified (Figure 1B&C), then the area of GFAP or NG2 staining (the number of pixels in which the intensity was above the set threshold) was divided by the total number of pixels in the area of the picture to yield GFAP or NG2 density.

The cross-sectional lesion area was calculated by counting the total number of pixels within the lesion as defined by the glial scar and a straight line connecting the dorsal surface of the injured spinal cord from 6 serial sections spaced 200μm apart for each rat. The total number of pixels was then converted into a physical area based on the relative size of the pixel. The relative size of each pixel at this magnification was determined to be 3.19×10^{-5} mm^2/pixel.

Macrophage/Microglia Immune Profile Analysis

To analyze the immune response, the lesion area was imaged at 40x magnification and individual 40x images of the lesion area were spliced together to yield a complete picture of the lesion area and surrounding intact cord. ED-1 staining of macrophages and microglia was analyzed surrounding the lesion site in 6 serial sections spaced 200μm apart from each rat to evaluate the immune response to the fibrin scaffolds. Immune response was analyzed by using a program written in the Matlab Image Processing Toolbox (Mathworks, Natick, MA). The program allowed the user to define the lesion border based on the GFAP stained lesion border as it was defined for the neural fiber density analysis. Based on this border, the program generates line profiles of a specific distance spaced 5μm apart originating at the lesion border and preceding either rostrally or caudally from the border. The program then analyzed the pixel intensity along this line and extracted relative ED-1 fluorescence intensity as a function of distance from the glial scar border 8. The analysis yielded an immune profile for each sample. To concisely convey this data, the normalized intensity was displayed at distances of 0, 50, 100, 200, and 400μm rostral (-) and caudal (+) to the lesion border.

Behavioral Analysis

Hindlimb function was assessed weekly after injury using the Basso, Beattie, and Bresnahan (BBB) locomotor rating scale in an open field (2 × 4 feet) and a grid walk test 18. For the BBB analysis, rats were videotaped for 4 min by ambulating on a non-slip surface, and each hindlimb was given a score by a blinded observer from 0 (no observable movements) to 21 (normal gait).

To complement the BBB analysis, a grid walk test was utilized. The grid walk test, which requires forelimb-hindlimb coordination, reveals deficits that are not apparent during normal locomotion, and thus was used to further evaluate the functional loss due to the dorsal hemisection model19. For this test, rats were videotaped while walking on a fixed grid of bars spaced 1 inch apart for 3 min. Footfalls, defined as missed steps resulting in the leg of the rat crossing the horizontal plane of the grid, were later counted during the allotted time on the grid by a blinded observer. The total number of footsteps taken on the grid was also counted. Using both counts, a percentage of missed steps was determined. The percentage of missed steps correlates inversely to functional recovery.

Statistical Analysis

All statistics were performed with Analysis of Variance (ANOVA, planned comparison post-hoc test, significant difference $p < 0.05$) using Statistica (StatSoft, Tulsa, OK).

Results

Fibrin Degradation and Fibrin Polymerization

For successful implementation of our treatment strategy it was necessary to identify the most efficient method for the incorporation of fibrin scaffolds into a subacute dorsal hemisection SCI. Two methods of fibrin scaffold polymerization were investigated to determine an effective method for polymerization and implantation of fibrin scaffolds within the injury site. The presence of fibrin scaffolds within the injury site was evaluated one week after implantation through the use of fluorescently conjugated fibrinogen. Fluorescent fibrin scaffolds were either allowed to polymerize partially into beads for 5 min at room temperature (Pre-Pol) prior to implantation (and gaps were filled with fibrin polymerized *in situ*) or the fluorescent fibrin pre-polymerization mixture was injected into the wound site for *in situ* polymerization (In Situ). After 7 days, scaffolds that were allowed to partially polymerize prior to implantation remained in the lesion site (Figure 2). Those scaffolds allowed to polymerize *in situ* could not be visualized and were assumed to have degraded by 7 days. Analysis of the neural fiber density within the lesion site, the astrocyte density surrounding the lesion site, and immune response to the fibrin scaffold showed no statistical difference between fibrin and untreated controls at 1 week after treatment (Figure 3).

Characteristics of the Lesion Site

In this study, a dorsal hemisection SCI model was used to target the dorsal motor tracts of the rat specifically, including the corticospinal tract and the rubrospinal tract. Following injury and treatment, cystic cavities, which are common after SCI, did not form in rats treated with fibrin scaffolds. Additionally, within the lesion area of the fibrin-treated groups, cell nuclei (Hoechst stained) were evenly dispersed throughout the lesion (Figure 4). The increased presence of cell nuclei within the lesion site suggests that treatment with fibrin scaffolds increased cell infiltration into the lesion site. In contrast to fibrin-treated groups, the untreated control groups often exhibited acellular regions within the lesion. The size of the lesion as defined by the GFAP staining was not significantly different between treated and untreated groups at 2 and 4 weeks after treatment ($p>0.05$) (Table 1).

Neural Fiber Density

The effect of fibrin scaffolds on neural fiber sprouting following subacute SCI was evaluated. Neural fiber density in the lesion site of each experimental group was quantified by analyzing the density of Tuj1 staining within the lesion site as defined by the glial scar border. The results show that the group treated with a pre-polymerized fibrin scaffold had significantly more neural fibers in the lesion site when compared to the untreated control group at both 2 and 4 weeks post treatment ($p<0.05$, $n=6$)) (Figure 5). There was no significant increase in neural fiber density at the 4 week time point of either group when compared to the 2 week time point of the same group (e.g. 2 week fibrin vs. 4 week fibrin). Sections from the group treated with fibrin scaffolds consistently exhibited Tuj1 positive neural fibers that extend past regions of GFAP staining and are found in the lesion at 2 and 4 weeks post implantation (Figure 6B). In contrast, Tuj1-positive neural fibers in the control group could frequently be seen closely associated with dense GFAP staining, failing to extend past the glial scar and into the lesion site (Figure 6A). The increased cellular infiltration in the fibrin-treated group correlated with a significant increase in neural fiber density defined by axons stained positive with Tuj1. These results demonstrate that treatment with fibrin scaffolds enhances neural fiber density within the lesion site following subacute SCI.

Astrocyte Density

Glial scarring following CNS damage has been associated with decreased axonal regeneration and decreased functional recovery. Astrocytes are the major component of the glial scar that forms following SCI, and may prevent regeneration following injury. In this study, we analyzed the density of astrocyte staining surrounding the injury site at 2 and 4 weeks following treatment with fibrin scaffolds. Two weeks following injury, the group treated with fibrin scaffolds had a significant decrease in the density of GFAP staining surrounding the injury site when compared to the untreated control group at both 2 and 4 weeks ($p<0.05$, 2 week fibrin treated vs. 2 and 4 week untreated controls, $n=6$ for each experimental group). The density at 2 weeks was ~21% in rats treated with fibrin scaffolds compared to ~33% measured in 2 and 4 week untreated control groups (Figure 7). GFAP density at 4 weeks in the fibrin-treated group was not significantly different from other experimental groups ($p>0.05$, 4 week fibrin vs. all experimental groups). These results suggest that the fibrin scaffolds delay the accumulation of GFAP positive astrocytes at the lesion border. Furthermore, in fibrin-treated groups at 2 weeks, GFAP staining was found in both the periphery and the center of the lesion, suggesting that the cells migrated from the lesion border into the lesion. Qualitatively, the overall GFAP staining within the lesion was lower in the untreated control group and the 4 week fibrin-treated group when compared to the 2 week fibrin treated group.

NG2 Density

CSPGs have been shown to prevent the regeneration of neural tissue following injury of the spinal cord. In this study, the density of CSPG surrounding the injury site was quantified following a subacute SCI. The density of NG2 staining surrounding the injury site in groups treated with fibrin scaffolds was not different from control groups ($p>0.1$) (Figure 8). Treatment with fibrin scaffolds did not alter NG2 deposition, which is associated with an increase in axonal regeneration inhibition. In the untreated control group at 2 and 4 weeks the area bordering the injury site was densely stained with NG2 and was accompanied by Tuj1 positive fibers that colocalized with the NG2 staining at the border, but did not extend into the lesion site. In contrast, the NG2 staining at the lesion border of the fibrin-treated group was more diffuse than controls and accompanied by Tuj1 positive fibers extending from the healthy tissue into the lesion site.

The deposition of NG2 seen in both experimental groups is consistent with deposition following SCI seen in other studies 20›21. Furthermore, NG2-labeled cells were observed frequently within the lesion site of the fibrin-treated groups, which suggests that these cells migrated from the host tissue into the lesion site. These NG2-positive cells within the lesion site were often colocalized with neural fibers that stained positively for Tuj1 (Figure 6).

Some of the labeled cells formed tubular structures that have been described previously22 as being associated with neo-vasculature (Figure 6). The tubular structures were seen in all of the sections from fibrin-treated animals at 2 and 4 weeks and in some of the control group at 4 weeks. The structures were not seen in the untreated control group at 2 weeks post treatment.

Macrophage/Microglia Immune Profile

The extent of immune response to an implanted material can have a significant effect on the intended function of the material. To evaluate the immune response of the transplanted fibrin scaffolds, a profile of macrophage/microglia presence adjacent to the lesion site was used to assess inflammation. As described in the methods, a program was developed that analyzed the immune profile of each experimental group. The immune profile is the intensity of ED-1 staining as a function of distance from the lesion border. In both the

untreated control and fibrin-treated groups, ED-1 positive cells accumulated at the lesion border. The fibrin scaffold treated groups contained small populations of ED-1 positive cells within the lesion site. The lesion site of the untreated control group lacked ED-1 staining and was largely acellular. Again, this observation demonstrates the ability of the fibrin scaffold to provide an environment permissive to cellular migration. Along the lesion border in both groups, a higher number of ED-1 positive cells were located within the grey matter along the lesion border (Figure 9). There was no difference between untreated control and fibrin-treated scaffold treated groups, which provides evidence that the fibrin scaffolds do not induce an increase in immune response following injury.

Functional recovery

The ability of fibrin scaffold to induce functional recovery following SCI was evaluated using the BBB locomotor function and grid walk functional test 18,19. Each experimental group showed spontaneous functional recovery over the time course of the study resulting in increases in BBB and a decrease in percentage of missed steps. However, the functional recovery was not statistically different between untreated control and fibrin-treated groups.

Discussion

Fibrin can provide a substrate for cells to proliferate and migrate, which makes it an ideal candidate for tissue engineering repair strategies. In this study, it was found that the treatment of SCI with fibrin scaffolds promoted the migration of cells and sprouting of neural fibers into the lesion site without eliciting an increased inflammatory response. It was found that pre-polymerizing fibrin scaffolds prior to implantation prolonged the presence of the fibrin scaffolds implanted *in vivo*. The degradation of fibrin scaffolds *in vivo* occurs predominantly through the actions of proteases such as plasmin 23-28. Absence of the *in situ* polymerized fibrin scaffold after one week may have resulted from the incorporation of endogenous plasminogen from the host during polymerization23,29. In contrast, those scaffolds pre-polymerized prior to implantation would incorporate minimal amount of plasminogen into the scaffold and thus would be less susceptible to bulk degradation by plasmin.

Thrombin concentration at the time of polymerization has been found to have an effect on fibrin scaffold structure and degradation30,31 and may have contributed to the absence of the *in situ* polymerized fibrin scaffolds in the injury site at 7 days. Fibrin scaffolds formed in the presence of low thrombin concentrations are composed of thick fibrin fibers and are highly susceptible to fibrinolysis, while scaffolds formed in the presence of high thrombin concentrations are composed of thin fibers and are relatively resistant to fibrinolysis 31. *In situ* polymerization in the presence of cerebral spinal fluid (in the injury site) may have diluted the concentration of thrombin, resulting in a scaffold that is structurally more susceptible to fibrinolysis. In contrast, the pre-polymerized fibrin scaffolds would have a consistent concentration of thrombin resulting in a more stable scaffold.

The interaction between the host tissue and the implanted scaffold is an important aspect of any biomaterial application. In this study, the injury site of the groups treated with fibrin scaffolds contained a uniform distribution of cell nuclei demonstrating the ability of fibrin to promote cellular migration into the lesion site (Figure 4). The ability of fibrin to promote cellular migration and infiltration has been seen with a variety of cell types during wound healing32,33. The increased cellular migration into fibrin scaffolds differs from some synthetic scaffolds, where severe astroglial scarring between host tissue and scaffold prevents cellular migration and axonal regeneration 8,9,11.

Dense astroglial scars that often form following SCI contain inhibitory molecules that can hinder the regeneration of axons34-36. It has been shown that the inhibitory nature of the astroglial scar can be overcome by the presence of growth promoting cues that serve to balance inhibitory cues from the glial scar22. We observed that treatment with fibrin scaffolds slows the accumulation of GFAP positive astrocytes at the lesion border (Figure 7). The delayed accumulation may provide a window where regeneration signals are stronger than inhibitory signals thus stimulating increased regeneration. Overall, the lesion border in the fibrin-treated group exhibited continuity of tissue across the lesion site as a result of the migration of cells into the lesion site.

The interactions between the fibrin scaffold and endogenous cells could either directly enhance axonal regeneration through direct interaction with neurons, or it could act by enhancing the migration of support cells that promote axonal regeneration. Human fibrinogen contains two Arg-Gly-Asp (RGD) sites, which provide sites for integrin binding 37. While, the direct interaction of neurons with fibrin RGD sites has not been thoroughly studied, others have shown evidence that neuronal growth can be stimulated by interaction between axons and other extracellular matrix proteins such as fibronectin 38-40. It has been shown that central nervous system neurons will adhere and extend neurites on fibronectin through interaction with the cell adhesion sequence RGD41. Likewise, fibronectin has been found to be a neuroprotectant following traumatic brain injury 42. In this way, it is conceivable that the adhesion between the fibrin scaffolds and host cells may contribute to the regeneration response observed in this study.

In the fibrin-treated group, there was an abundance of NG2 positive cells within the lesion site. The CSPG NG2 has been shown to be expressed on oligodendrocyte progenitor cells, Schwann cells, endothelial cells, and macrophages20,22,43-46. In the present study, NG2 positive cells were observed surrounding or ensheathing neural fibers (Figure 6). This is consistent with the literature where cells staining positive for NG2 were seen ensheathing axons within the lesion site following SCI 22. Other NG2 positive cells within the lesion site of the fibrin-treated groups formed tubular “blood vessel-like” structures (Figure 6). These tubular structures formed by NG2 positive cells, have been described previously22, and their presence suggests that the environment within the lesion site of fibrin-treated group may be vascularized.

As seen in this study and others, crushed or transected nerve fibers of the CNS exhibit regenerative potential following injury47. However, in the CNS as the injury matures regeneration is stifled by inhibitory cues. The stifled regeneration then leads to degeneration of severed axons, which is observed in rodents for months following SCI48. Consistent with this pathophysiology, the untreated control group in this study exhibited an increase in neural fiber density between 1 and 2 weeks followed by a decrease in density between 2 and 4 weeks. In contrast, the neural fiber density seen in the fibrin-treated group significantly increased between 1 and 2 weeks and was maintained between 2 and 4 weeks. These results suggest that the balance of inhibitory cues, which surrounds the injury site, was outweighed by the presence of permissive regenerative cues within the lesion site for the fibrin-treated group.

In this study, it was observed that the density of astrocytes surrounding the lesion in the fibrin-treat group was decreased at 2 weeks. Previously, it has been shown that glial cells readily migrate into fibrin matrices49. Increased migration of glial cells into the lesion site may have lead to the decrease in astrocyte density surrounding the lesion site observed in our study. Previously, it has been found, that reducing or removing inhibitory components within the glial scar following SCI increased axonal regeneration50,51. Likewise, the decrease in astrocyte density in our study could have increased the ability of axons to extend

into the lesion site by reducing the strength of the inhibitory signals present. Additionally, others have shown that elongated glial processes that cross the lesion border, such as those seen in fibrin-treated group (Figure 6), provide a more permissive environment for axonal sprouting14.

The results of this study suggest that fibrin scaffolds can enhance host cell proliferation and axonal regeneration in the central nervous system at subacute time points following SCI. Although there was a lack of difference in functional recovery between experimental groups, it should be noted that the time points in this study are relatively short for the evaluation of functional recovery. Future work will investigate the effect of fibrin scaffolds in combination with other treatment methods such as protein delivery and cell transplantation on spinal cord regeneration following injury.

Acknowledgments

The authors acknowledge Dan Hunter for assistance with tissue preparation and image analysis, and Angela Guzmán for assistance with animal care. This study was supported by NIH R01 NS051454.

References

1. Fawcett JW, Asher RA. The glial scar and central nervous system repair. Brain Res Bull. 1999; 49(6):377–91. [PubMed: 10483914]
2. McDonald JW, Sadowsky C. Spinal-cord injury. Lancet. 2002; 359(9304):417–25. [PubMed: 11844532]
3. Hagg T, Oudega M. Degenerative and spontaneous regenerative processes after spinal cord injury. J Neurotrauma. 2006; 23(3-4):264–80. [PubMed: 16629615]
4. Raghow R. The role of extracellular matrix in postinflammatory wound healing and fibrosis. Faseb J. 1994; 8(11):823–31. [PubMed: 8070631]
5. Dam-Hieu P, Liu S, Choudhri T, Said G, Tadie M. Regeneration of primary sensory axons into the adult rat spinal cord via a peripheral nerve graft bridging the lumbar dorsal roots to the dorsal column. J Neurosci Res. 2002; 68(3):293–304. [PubMed: 12111859]
6. Decherchi P, Gauthier P. Regrowth of acute and chronic injured spinal pathways within supra-lesional post-traumatic nerve grafts. Neuroscience. 2000; 101(1):197–210. [PubMed: 11068148]
7. Geller HM, Fawcett JW. Building a bridge: engineering spinal cord repair. Exp Neurol. 2002; 174(2):125–36. [PubMed: 11922655]
8. Jain A, Kim YT, McKeon RJ, Bellamkonda RV. In situ gelling hydrogels for conformal repair of spinal cord defects, and local delivery of BDNF after spinal cord injury. Biomaterials. 2006; 27(3): 497–504. [PubMed: 16099038]
9. Hurtado A, Moon LD, Maquet V, Blits B, Jerome R, Oudega M. Poly (D,L-lactic acid) macroporous guidance scaffolds seeded with Schwann cells genetically modified to secrete a bi-functional neurotrophin implanted in the completely transected adult rat thoracic spinal cord. Biomaterials. 2006; 27(3):430–42. [PubMed: 16102815]
10. Stokols S, Tuszynski MH. Freeze-dried agarose scaffolds with uniaxial channels stimulate and guide linear axonal growth following spinal cord injury. Biomaterials. 2006; 27(3):443–51. [PubMed: 16099032]
11. Woerly S, Pinet E, de Robertis L, Van Diep D, Bousmina M. Spinal cord repair with PHPMA hydrogel containing RGD peptides (NeuroGel). Biomaterials. 2001; 22(10):1095–111. [PubMed: 11352090]
12. Currie LJ, Sharpe JR, Martin R. The use of fibrin glue in skin grafts and tissue-engineered skin replacements: a review. Plast Reconstr Surg. 2001; 108(6):1713–26. [PubMed: 11711954]
13. Lee AC, Yu VM, Lowe JB 3rd, Brenner MJ, Hunter DA, Mackinnon SE, Sakiyama-Elbert SE. Controlled release of nerve growth factor enhances sciatic nerve regeneration. Exp Neurol. 2003; 184(1):295–303. [PubMed: 14637100]

14. Taylor SJ, Rosenzweig ES, McDonald JW 3rd, Sakiyama-Elbert SE. Delivery of neurotrophin-3 from fibrin enhances neuronal fiber sprouting after spinal cord injury. J Control Release. 2006; 113(3):226–35. [PubMed: 16797770]
15. Sakiyama-Elbert SE, Hubbell JA. Controlled release of nerve growth factor from a heparin-containing fibrin-based cell ingrowth matrix. J Control Release. 2000; 69(1):149–58. [PubMed: 11018553]
16. Sakiyama-Elbert SE, Hubbell JA. Development of fibrin derivatives for controlled release of heparin-binding growth factors. J Control Release. 2000; 65(3):389–402. [PubMed: 10699297]
17. Schense JC, Hubbell JA. Cross-linking exogenous bifunctional peptides into fibrin gels with factor XIIIa. Bioconjug Chem. 1999; 10(1):75–81. [PubMed: 9893967]
18. Basso DM, Beattie MS, Bresnahan JC. A sensitive and reliable locomotor rating scale for open field testing in rats. J Neurotrauma. 1995; 12(1):1–21. [PubMed: 7783230]
19. Metz GA, Merkler D, Dietz V, Schwab ME, Fouad K. Efficient testing of motor function in spinal cord injured rats. Brain Res. 2000; 883(2):165–77. [PubMed: 11074045]
20. Jones LL, Yamaguchi Y, Stallcup WB, Tuszynski MH. NG2 is a major chondroitin sulfate proteoglycan produced after spinal cord injury and is expressed by macrophages and oligodendrocyte progenitors. J Neurosci. 2002; 22(7):2792–803. [PubMed: 11923444]
21. Tan AM, Colletti M, Rorai AT, Skene JH, Levine JM. Antibodies against the NG2 proteoglycan promote the regeneration of sensory axons within the dorsal columns of the spinal cord. J Neurosci. 2006; 26(18):4729–39. [PubMed: 16672645]
22. Lu P, Jones LL, Tuszynski MH. Axon regeneration through scars and into sites of chronic spinal cord injury. Exp Neurol. 2007; 203(1):8–21. [PubMed: 17014846]
23. Francis CW, Marder VJ. Concepts of clot lysis. Annu Rev Med. 1986; 37:187–204. [PubMed: 2939790]
24. Herbert CB, Bittner GD, Hubbell JA. Effects of fibinolysis on neurite growth from dorsal root ganglia cultured in two- and three-dimensional fibrin gels. J Comp Neurol. 1996; 365(3):380–91. [PubMed: 8822177]
25. Herbert CB, Nagaswami C, Bittner GD, Hubbell JA, Weisel JW. Effects of fibrin micromorphology on neurite growth from dorsal root ganglia cultured in three-dimensional fibrin gels. J Biomed Mater Res. 1998; 40(4):551–9. [PubMed: 9599031]
26. Werb Z. ECM and cell surface proteolysis: regulating cellular ecology. Cell. 1997; 91(4):439–42. [PubMed: 9390552]
27. Vu TH, Werb Z. Matrix metalloproteinases: effectors of development and normal physiology. Genes Dev. 2000; 14(17):2123–33. [PubMed: 10970876]
28. Sternlicht MD, Bissell MJ, Werb Z. The matrix metalloproteinase stromelysin-1 acts as a natural mammary tumor promoter. Oncogene. 2000; 19(8):1102–13. [PubMed: 10713697]
29. Smith JD, Chen A, Ernst LA, Waggoner AS, Campbell PG. Immobilization of aprotinin to fibrinogen as a novel method for controlling degradation of fibrin gels. Bioconjug Chem. 2007; 18(3):695–701. [PubMed: 17432824]
30. Carr ME Jr. Gabriel DA, McDonagh J. Influence of Ca2+ on the structure of reptilase-derived and thrombin-derived fibrin gels. Biochem J. 1986; 239(3):513–6. [PubMed: 3548699]
31. Wolberg AS. Thrombin generation and fibrin clot structure. Blood Rev. 2007; 21(3):131–42. [PubMed: 17208341]
32. Cox S, Cole M, Tawil B. Behavior of human dermal fibroblasts in three-dimensional fibrin clots: dependence on fibrinogen and thrombin concentration. Tissue Eng. 2004; 10(5-6):942–54. [PubMed: 15265312]
33. Lin F, Ren XD, Doris G, Clark RA. Three-dimensional migration of human adult dermal fibroblasts from collagen lattices into fibrin/fibronectin gels requires syndecan-4 proteoglycan. J Invest Dermatol. 2005; 124(5):906–13. [PubMed: 15854029]
34. Prang P, Muller R, Eljaouhari A, Heckmann K, Kunz W, Weber T, Faber C, Vroemen M, Bogdahn U, Weidner N. The promotion of oriented axonal regrowth in the injured spinal cord by alginate-based anisotropic capillary hydrogels. Biomaterials. 2006; 27(19):3560–9. [PubMed: 16500703]

35. Patist CM, Mulder MB, Gautier SE, Maquet V, Jerome R, Oudega M. Freeze-dried poly(D,L-lactic acid) macroporous guidance scaffolds impregnated with brain-derived neurotrophic factor in the transected adult rat thoracic spinal cord. Biomaterials. 2004; 25(9):1569–82. [PubMed: 14697859]
36. Hsu JY, Xu XM. Early profiles of axonal growth and astroglial response after spinal cord hemisection and implantation of Schwann cell-seeded guidance channels in adult rats. J Neurosci Res. 2005; 82(4):472–83. [PubMed: 16240391]
37. Mosesson MW. Fibrinogen and fibrin structure and functions. J Thromb Haemost. 2005; 3(8): 1894–904. [PubMed: 16102057]
38. Ju YE, Janmey PA, McCormick ME, Sawyer ES, Flanagan LA. Enhanced neurite growth from mammalian neurons in three-dimensional salmon fibrin gels. Biomaterials. 2007; 28(12):2097–108. [PubMed: 17258313]
39. King VR, Henseler M, Brown RA, Priestley JV. Mats made from fibronectin support oriented growth of axons in the damaged spinal cord of the adult rat. Exp Neurol. 2003; 182(2):383–98. [PubMed: 12895449]
40. King VR, Phillips JB, Hunt-Grubbe H, Brown R, Priestley JV. Characterization of non-neuronal elements within fibronectin mats implanted into the damaged adult rat spinal cord. Biomaterials. 2006; 27(3):485–96. [PubMed: 16102813]
41. Rogers SL, Letourneau PC, Peterson BA, Furcht LT, McCarthy JB. Selective interaction of peripheral and central nervous system cells with two distinct cell-binding domains of fibronectin. J Cell Biol. 1987; 105(3):1435–42. [PubMed: 2958484]
42. Tate CC, Garcia AJ, Laplaca MC. Plasma fibronectin is neuroprotective following traumatic brain injury. Exp Neurol. 2007; 207(1):13–22. [PubMed: 17599836]
43. Jones LL, Sajed D, Tuszynski MH. Axonal regeneration through regions of chondroitin sulfate proteoglycan deposition after spinal cord injury: a balance of permissiveness and inhibition. J Neurosci. 2003; 23(28):9276–88. [PubMed: 14561854]
44. Yoo S, Wrathall JR. Mixed primary culture and clonal analysis provide evidence that NG2 proteoglycan-expressing cells after spinal cord injury are glial progenitors. Dev Neurobiol. 2007; 67(7):860–74. [PubMed: 17506499]
45. Ong WY, Levine JM. A light and electron microscopic study of NG2 chondroitin sulfate proteoglycan-positive oligodendrocyte precursor cells in the normal and kainate-lesioned rat hippocampus. Neuroscience. 1999; 92(1):83–95. [PubMed: 10392832]
46. McTigue DM, Wei P, Stokes BT. Proliferation of NG2-positive cells and altered oligodendrocyte numbers in the contused rat spinal cord. J Neurosci. 2001; 21(10):3392–400. [PubMed: 11331369]
47. Taylor SJ, McDonald JW 3rd, Sakiyama-Elbert SE. Controlled release of neurotrophin-3 from fibrin gels for spinal cord injury. J Control Release. 2004; 98(2):281–94. [PubMed: 15262419]
48. David S. Recruiting the immune response to promote long distance axon regeneration after spinal cord injury. Prog Brain Res. 2002; 137:407–14. [PubMed: 12440383]
49. Knoops B, Hubert I, Hauw JJ, van den Bosch de Aguilar P. Axonal growth and glial migration from co-cultured hippocampal and septal slices into fibrin-fibronectin-containing matrix of peripheral regeneration chambers: a light and electron microscope study. Brain Res. 1991; 540(1-2):183–94. [PubMed: 2054610]
50. Bradbury EJ, Moon LD, Popat RJ, King VR, Bennett GS, Patel PN, Fawcett JW, McMahon SB. Chondroitinase ABC promotes functional recovery after spinal cord injury. Nature. 2002; 416(6881):636–40. [PubMed: 11948352]
51. Barritt AW, Davies M, Marchand F, Hartley R, Grist J, Yip P, McMahon SB, Bradbury EJ. Chondroitinase ABC promotes sprouting of intact and injured spinal systems after spinal cord injury. J Neurosci. 2006; 26(42):10856–67. [PubMed: 17050723]

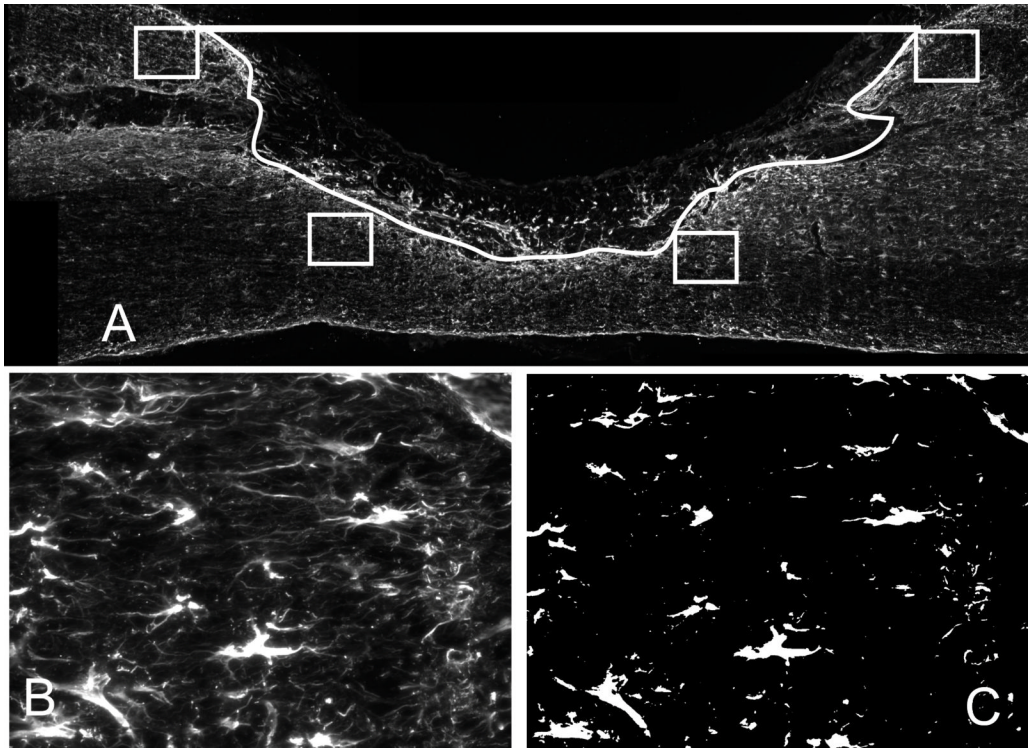

Figure 1.
The lesion was defined in each section by a line connecting the dorsal surface of the cord and a trace of the glial scar based on GFAP staining. A) Image of a section from the 1 week control group stained with GFAP. The lesion is outlined in white (excluding the square box) and the lesion area was defined as the space within this outline. The four small boxes in A) are representative of the four locations (2 rostral and 2 caudal) on each section that are imaged to analyze GFAP and NG2 density surrounding the cord. B) Representative 200x image of GFAP staining from small boxed region. C) Each 200x GFAP (or NG2) image was set to a threshold such that only positive staining for GFAP (or NG2) was observed. The total number of pixels positive for GFAP (or NG2) was then divided by the total number of pixels from the image yielding GFAP density.

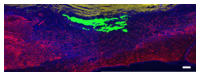

Figure 2.
Fibrin scaffold in the lesion site 1 week after implantation. Fluorescently labeled fibrinogen was used to evaluate the presence of fibrin scaffolds 1 week after implantation of subacute SCI using two different polymerization methods (pre-polymerized and *in situ* polymerized). In the groups treated with a pre-polymerized fibrin (Pre Pol), 1 week following implantation the fluorescently labeled fibrin scaffolds could be visualized in the lesion site. Image of a sagittal section from the Pre Pol group showing neural fibers (Tuj1, red), cell nuclei (Hoechst, blue), artificial dura (yellow, dorsal aspect of the sagittal section) and pre-polymerized fibrin scaffold (green). Those groups treated with *in situ* polymerized fibrin scaffolds, the scaffolds were not visible at 1 week following implantation. (Scale bar = 200μm)

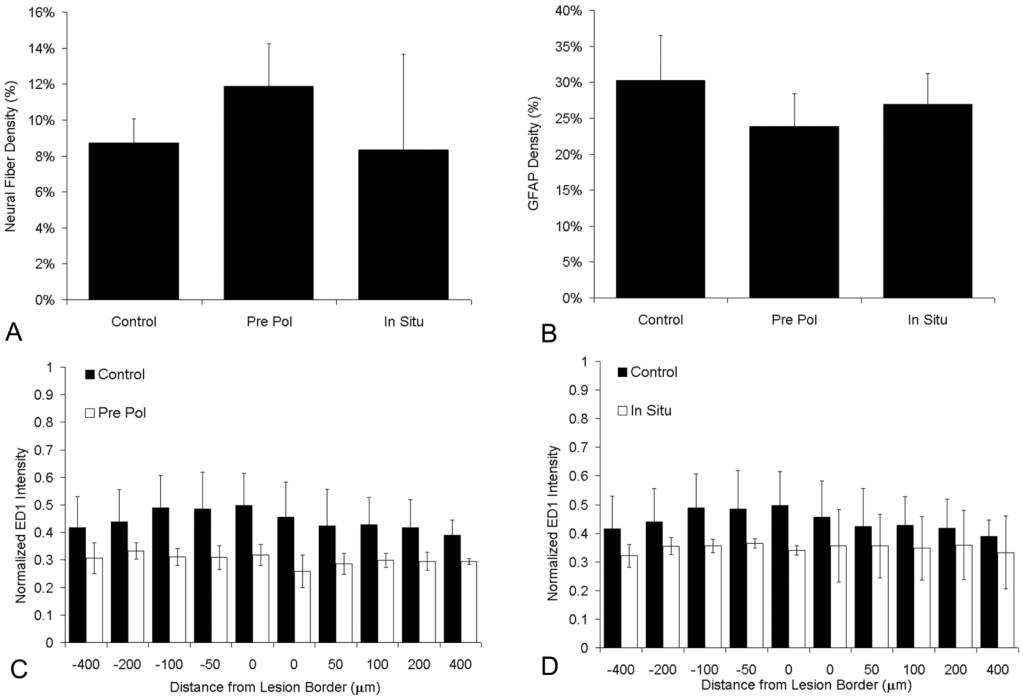

Figure 3.

Immunohistochemical analysis of sections from each polymerization method. The effect of treatment with pre-polymerized fibrin scaffolds (Pre Pol), *in situ* polymerized fibrin scaffolds (In Situ) and untreated control (Control) on the density of neural fiber (Tuj1)density in the lesion site, astrocyte staining (GFAP) density surrounding the lesion site, and immune response, based on ED1 staining, as a function of distance from the lesion border. A) Neural fiber (Tuj1) density of control, Pre Pol, and In Situ groups 1 week after implantation. B) GFAP density surrounding the lesion site of control, Pre Pol, and In Situ groups 1 week after implantation. C) ED1 intensity with respect to distance away from the lesion border in response to untreated control, and Pre Pol fibrin scaffolds. The normalized intensity is displayed at distances of 0, 50, 100, 200, and 400μm rostral (-) and caudal (+) to the lesion border. D) ED1 intensity with respect to distance away from the lesion border in response to untreated control, and In Situ fibrin scaffolds 1 week after implantation. The normalized intensity is displayed at distances of 0, 50, 100, 200, and 400μm rostral (-) and caudal (+) to the lesion border. (Error bars (A,B) and error bars (C, D) represent standard deviation, n=3 for each experimental group)

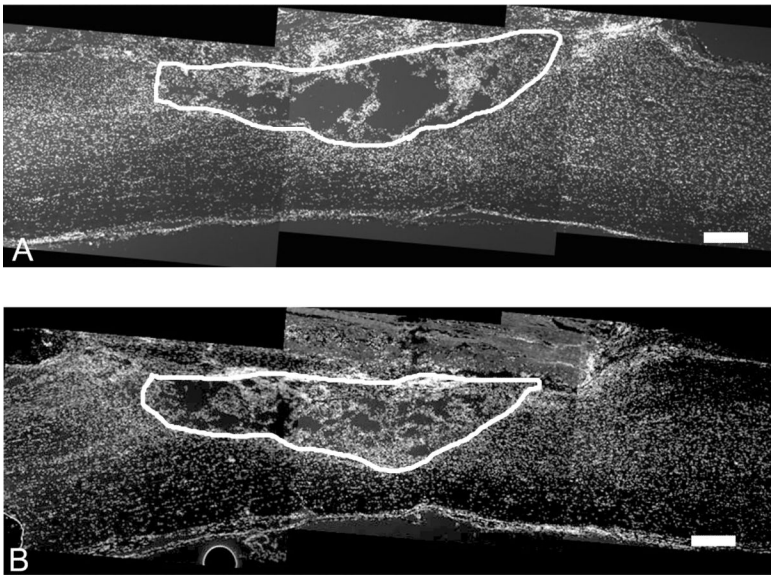

Figure 4.

Nuclear staining of sagittal sections of lesion area of A) untreated control B) fibrin-treated group 2 weeks after treatment of subacute SCI. White line on the sections outlines the lesion border. Lesions from the fibrin-treated group (B) have more cell nuclei compared to untreated controls (A). (Scale bar = 200μm)

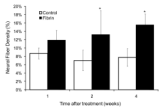

Figure 5.
Neural fiber density within the lesion site. Fibrin scaffolds enhanced neural fiber density within the lesion site 2 and 4 weeks following implantation when compared to untreated control groups at the same time point. (Error bars represent standard deviation, * denotes $p < 0.05$ versus untreated control)

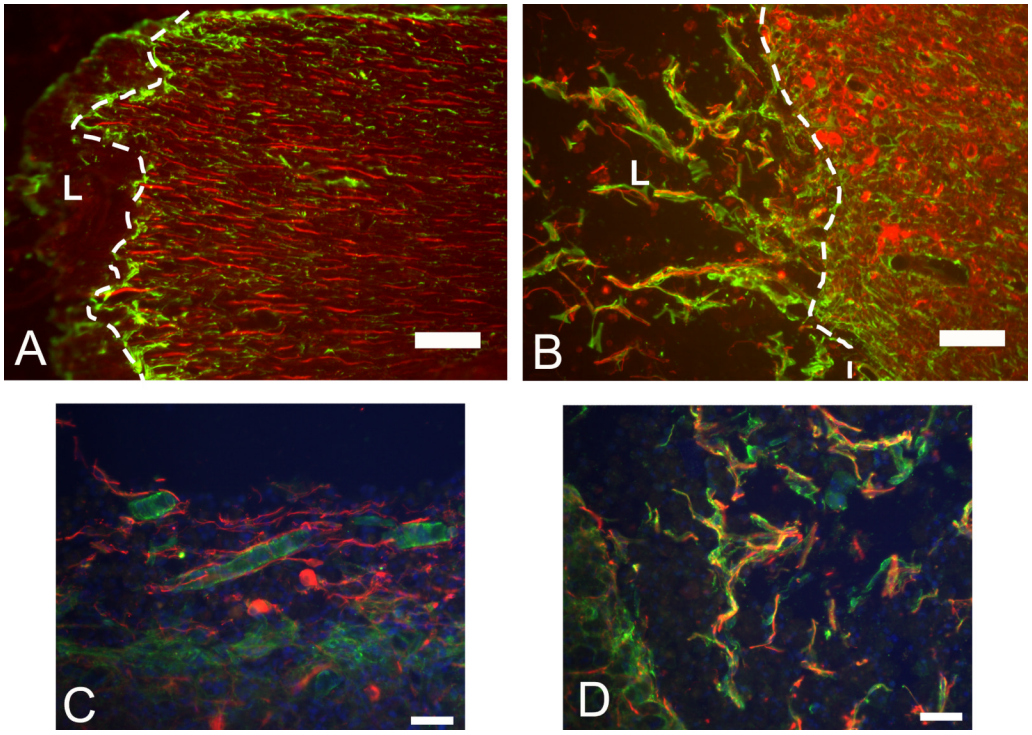

Figure 6.
Staining of neural fibers, astrocytes, and NG2 CSPGs. Images (A and B) of the lesion border stained with Tuj1 (red) and GFAP (green). White dashed line indicates glial border and "L" indicates lesion site. A) The lesion border from the 4 week untreated control group showing neural fibers associated with the glial border and that do not extend past the border. B) Image of the lesion border from the 4 week fibrin-treated group showing neural fibers that extend past the glial border and are found in the lesion. The neural fibers are accompanied by elongated glial processes of GFAP positive astrocytes that accompany the neural fibers into the lesion site. C) The image of NG2 positive tubular structures (Green) in close association with Tuj1 positive neurons (Red). NG2 positive cells were also seen to co-localize and surround neural fibers that stained positively for Tuj1. D) The image co-localization of NG2 staining (Green) and Tuj1 staining (Red) resembling myelination of neural fibers (scale bar = 100μm).

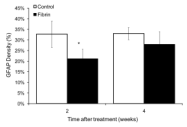

Figure 7.

Effect of fibrin scaffolds on astrocyte density. Fibrin scaffolds decreased the density of astrocyte staining surrounding the lesion site 2 weeks following implantation into the lesion site. The groups treated with fibrin scaffolds had a significant decrease in astrocyte staining surrounding the lesion site when compared to control groups (Error bars represent standard deviation, * denotes $p < 0.05$ versus untreated control).

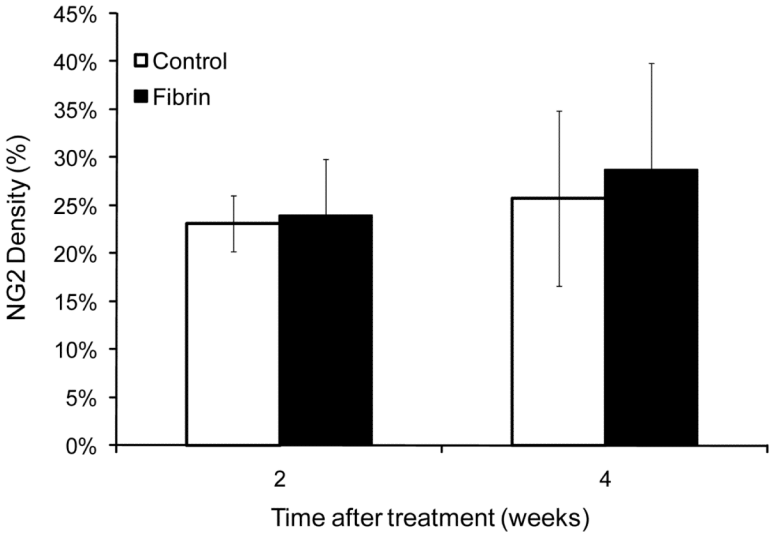

Figure 8.

Effect of fibrin scaffolds on chondroitin sulfate proteoglycan (NG2) density. NG2 density surrounding the lesion site for the control and fibrin treated groups at 2 and 4 weeks following treatment. No significant difference was observed in NG2 density surrounding the lesion site between untreated control groups and fibrin-treated groups. (Error bars represent standard deviation).

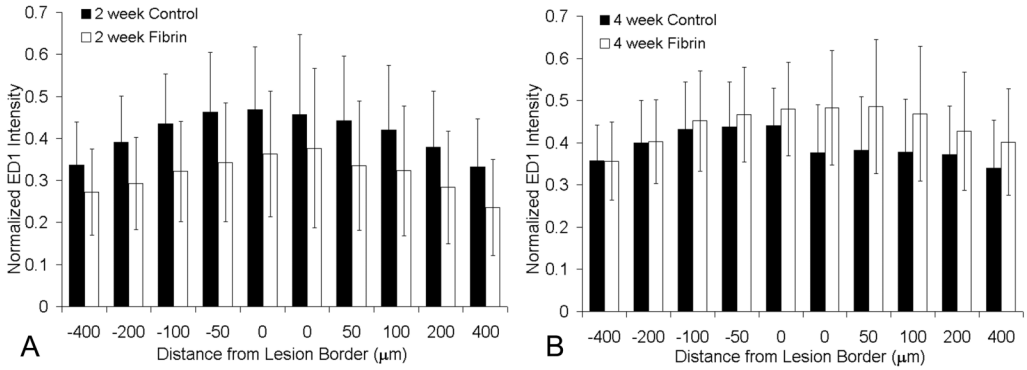

Figure 9.

Effect of fibrin scaffold on macrophage/microglia staining. Immune response to the fibrin scaffolds was analyzed by measuring the intensity of ED1 staining as a function of distance from the lesion border. The analysis yielded an immune profile for each experimental group that was normalized by a positive control. A) ED1 profile for the control (black bars) and fibrin treated groups (white bars) 2 weeks following implantation. The normalized intensity is displayed at distances of 0, 50, 100, 200, and 400μm rostral (-) and caudal (+) to the lesion border. The experimental groups were not statistically different at any distance in the 2 week time point ($p>0.05$). B) ED1 profile of the control and fibrin treated groups 4 weeks following implantation. The normalized intensity is displayed at distances of 0, 50, 100, 200, and 400μm rostral (-) and caudal (+) to the lesion border. The experimental groups were not statistically different at any distance in the 4 week time point ($p>0.05$) (error bars represent standard deviation).

Table 1

	Cross Sectional Lesion Area (mm^2)	
Time point	2 week	4 week
Control	1.82±0.71	1.22±0.39
Fibrin Pre-Pol	1.84±0.67	1.60±0.49